

Citation for published version:

Radeck, J, Gebhard, S, Orchard, PS, Kirchner, M, Bauer, S, Mascher, T & Fritz, G 2016, 'Anatomy of the bacitracin resistance network in *Bacillus subtilis*', *Molecular Microbiology*, vol. 100, no. 4, pp. 607-620.
<https://doi.org/10.1111/mmi.13336>

DOI:

[10.1111/mmi.13336](https://doi.org/10.1111/mmi.13336)

Publication date:

2016

Document Version

Peer reviewed version

[Link to publication](#)

Publisher Rights

Unspecified

This is the peer reviewed version of the following article: Radeck, J, Gebhard, S, Orchard, P, Kirchner, M, Bauer, S, Mascher, T & Fritz, G 2016, 'Anatomy of the bacitracin resistance network in *Bacillus subtilis*' *Molecular Microbiology*. which has been published in final form at <http://dx.doi.org/10.1111/mmi.13336>. This article may be used for non-commercial purposes in accordance with Wiley Terms and Conditions for Self-Archiving.

University of Bath

General rights

Copyright and moral rights for the publications made accessible in the public portal are retained by the authors and/or other copyright owners and it is a condition of accessing publications that users recognise and abide by the legal requirements associated with these rights.

Take down policy

If you believe that this document breaches copyright please contact us providing details, and we will remove access to the work immediately and investigate your claim.

Anatomy of the bacitracin resistance network in *Bacillus subtilis*

Jara Radeck^{1,2}, Susanne Gebhard³, Peter Shevlin Orchard², Marion Kirchner^{2,†},
Stephanie Bauer², Thorsten Mascher^{1*} and Georg Fritz⁴

¹ Technische Universität Dresden, Institute of Microbiology, Dresden, Germany

² Ludwig-Maximilians-Universität München, Department Biology I, München, Germany

³ University of Bath, Milner Centre for Evolution, Department of Biology and Biochemistry, Bath, UK

⁴ Philipps-Universität Marburg, LOEWE-Center for Synthetic Microbiology (SYNMIKRO), Marburg, Germany

[†]Present affiliation: Technische Universität München, Department of Chemistry, Garching, Germany

*For correspondence: Email thorsten.mascher@tu-dresden.de; Tel. (+49) 351 463-40420; Fax (+49) 351 463-37715

Abstract

Protection against antimicrobial peptides (AMPs) often involves the parallel production of multiple, well-characterized resistance determinants. So far, little is known about how these resistance modules interact and how they jointly protect the cell. Here, we studied the interdependence between different layers of the envelope stress response of *Bacillus subtilis* when challenged with the lipid II cycle-inhibiting AMP bacitracin. The underlying regulatory network orchestrates the production of the ABC transporter BceAB, the UPP phosphatase BcrC and the phage-shock proteins LialH. Our systems-level analysis reveals a clear hierarchy, allowing us to discriminate between primary (BceAB) and secondary (BcrC and LialH) layers of bacitracin resistance. Deleting the primary layer provokes an enhanced induction of the secondary layer to partially compensate for this loss. This study reveals a direct role of LialH in bacitracin resistance, provides novel insights into the feedback regulation of the Lia system, and demonstrates a pivotal role of BcrC in maintaining cell wall homeostasis. The compensatory regulation within the bacitracin network can also explain how gene expression noise propagates between resistance layers. We suggest that this active redundancy in the bacitracin resistance network of *B. subtilis* is a general principle to be found in many bacterial antibiotic resistance networks.

Keywords

PspA, phage-shock protein, antibiotic resistance, envelope stress response, signal transduction, gene regulation

Introduction

In their natural environment many microbes are in fierce competition for a limited supply of resources. This frequently involves the production of antimicrobial peptides (AMPs) that suppress the proliferation of competitors (Eijsink *et al.*, 2002). In this biochemical warfare, the cell envelope serves as a prime target, and many AMPs interfere with its biosynthesis and integrity (Breukink and de Kruijff, 2006). To defend against antimicrobial attacks by rival species, it is thus of vital importance for cells to accurately sense these cues and to swiftly mount protective countermeasures, collectively referred to as cell envelope stress response (CESR) (Jordan *et al.*, 2008; Schrecke *et al.*, 2012). In many bacteria the defense against AMPs involves the simultaneous expression of a number of resistance systems that protect cells at various levels. Those include on the one hand specific resistance determinants, such as ABC transporters (Gebhard, 2012) and immunity lipoproteins (Stein *et al.*, 2003; Aso *et al.*, 2005) that transport and/or sequester AMPs from their molecular targets. On the other hand, bacteria induce the production of more nonspecific resistance determinants that alter the charge and composition of the cell envelope to reduce access of AMPs to their sites of action (Revilla-Guarinos *et al.*, 2014) and allow cells to cope with deleterious effects on downstream cell physiology (Joly *et al.*, 2010). While many of the AMP resistance modules have been individually characterized in great detail, our present knowledge about how these modules interact, and how they jointly contribute to the overall AMP resistance of a cell, is still limited. Thus, as for many other bacterial stress responses, the daunting task is to decipher how the cell orchestrates the activity of individual resistance modules into a complex and multi-layered CESR network.

In the present work we approached this question by focusing on the resistance mechanisms of *Bacillus subtilis* against the peptide antibiotic bacitracin, which is produced by some strains of *Bacillus licheniformis* and *B. subtilis* (Azevedo *et al.*, 1993; Ishihara *et al.*, 2002) and is clinically used as broad spectrum antibiotic against Gram-positive bacteria causing skin infections. Bacitracin acts by inhibiting the lipid II cycle of cell wall biosynthesis, which is essential for the translocation of peptidoglycan precursors from the cytosol to the extracytoplasmic space (Fig. 1A). The tight complex formation between bacitracin and the diphosphate lipid carrier undecaprenyl pyrophosphate (UPP) prevents dephosphorylation of UPP to undecaprenyl phosphate (UP) and thereby efficiently blocks recycling of the lipid carrier (Storm and Strominger, 1973; Economou *et al.*, 2013).

To perpetuate progression of the lipid II cycle under bacitracin attack and to protect against cell envelope damage, *B. subtilis* up-regulates the expression of three major resistance modules (Mascher *et al.*, 2003; Rietkötter *et al.*, 2008): The ABC transporter BceAB (Ohki *et al.*, 2003; Mascher *et al.*, 2003), the UPP phosphatase BcrC (Cao and Helmann, 2002; Ohki *et al.*,

2003; Bernard *et al.*, 2005) and the phage shock protein (Psp)-like LiaI and LiaH proteins (Mascher *et al.*, 2004; Jordan *et al.*, 2006) (Fig. 1A and B). Recent evidence suggests that BceAB confers resistance by clearing UPP from the inhibitory grip of bacitracin (Fritz *et al.*, 2015), but it remains elusive whether bacitracin is transported into the cytoplasm for degradation or whether it is released into the extracytoplasmic space, as suggested previously (Rietkötter *et al.*, 2008; Ohki *et al.*, 2003). Simultaneously, the phosphatase BcrC catalyzes the dephosphorylation of UPP to UP (Fig. 1A) and thereby promotes the progression of the Lipid II cycle. Finally, under cell-envelope perturbing conditions the *liaIH* operon is induced, and the small membrane anchor protein LiaI recruits the cytosolic PspA/IM30 protein family member LiaH into static, membrane-associated patches (Domínguez-Escobar *et al.*, 2014). While the homologous Psp system encoded by the *pspABCDE* operon of *Escherichia coli* has been linked to maintenance of the proton motive force under envelope-perturbing conditions (Kleerebezem *et al.*, 1996; Kobayashi *et al.*, 2007), the physiological role of the Lia system in *B. subtilis* remained elusive: despite its more than ~100-fold induction under bacitracin stress, no increase in bacitracin sensitivity was detected in a *liaIH* deletion strain (Wolf *et al.*, 2010). While this might suggest that there is no contribution of the Lia system to bacitracin resistance, we reasoned that the presence of the two other bacitracin resistance layers, BceAB and BcrC, could potentially compensate for the lack of LiaH. However, to date it is not known whether these systems act in fact redundantly, or whether they contribute independently or even cooperatively to bacitracin resistance.

To gain deeper insight into how these modules interact and form an efficient bacitracin stress response network, we here systematically studied their functional and regulatory interactions in a comprehensive set of mutants deficient in the three resistance determinants. Our analysis reveals a hierarchy among resistance modules, which we find reflected in marked anti-correlations between the expression of primary (drug-sensing) and secondary (mostly damage-sensing) layers of bacitracin resistance. This means that the increased expression of the primary resistance layer reduced the expression of the secondary layer and *vice versa*. Strikingly, these anti-correlations can also explain how gene expression noise propagates between the different resistance modules at the single cell level, as revealed by flow cytometry analyses. Moreover, our study underpins the importance of the UPP phosphatase BcrC for cell wall homeostasis in the absence of bacitracin stress and provides novel clues about the physiological stimuli triggering the induction of the modules in the bacitracin resistance network.

Results

Contributions of CESR modules to antibiotic resistance

First, we studied whether the three CESR modules protect the cell in a redundant, independent or even in a cooperative manner. To this end we constructed mutants deficient in one, two or in all three resistance determinants and determined their sensitivity towards bacitracin using the E-test[®] agar gradient diffusion method (Fig. 2A). Compared to the minimal inhibitory concentration (MIC) of bacitracin for wild type cells (256 µg/ml), mutants deficient in only one of the resistance modules displayed a clear hierarchy in their sensitivity towards bacitracin: While the MIC of the Δ *lialH* mutant was identical to that of the wild type, the Δ *bcrC* mutant displayed a 5-fold and the Δ *bceAB* mutant an 85-fold increase in bacitracin susceptibility, suggesting that BceAB acts as the primary resistance determinant under these growth conditions. Interestingly, in a mutant background devoid of *bceAB*, the additional deletion of either of the other two resistance modules had a significantly stronger impact on the MIC than observed in the single mutants. Here, the Δ *bceAB* Δ *lialH* double mutant had a 6-fold lower MIC than the Δ *bceAB* mutant, thereby revealing the first phenotype of LialH in the bacitracin stress response. Hence, we suggest that the previously reported lack of a Δ *lialH* phenotype upon bacitracin stress (Rietkötter *et al.*, 2008) might be explained by a redundant organization of the bacitracin stress response network, in which resistance conferred by BceAB masks the weaker contribution of the LialH module. Moreover, the Δ *bceAB* Δ *bcrC* double mutant was 24-fold more sensitive than the Δ *bceAB* reference strain, suggesting that BceAB also partially masks the contribution of BcrC. Please note that we did not observe a similar “masking effect” between the secondary resistance modules, as the MIC of a Δ *bcrC* mutant (48 µg/ml) was identical to that of a Δ *bcrC* Δ *lialH* mutant (Fig. 2A). Only when compared to a Δ *bceAB* Δ *bcrC* double mutant, we found that a Δ *bceAB* Δ *bcrC* Δ *lialH* triple mutant showed an ~3-fold increased bacitracin sensitivity (Fig. 2A). In summary, these results show that the secondary resistance modules do in fact protect the cell against bacitracin, but also reveal that the contributions of the secondary resistance modules are masked by the much stronger resistance conferred by the Bce system.

Next, we asked whether the increased bacitracin susceptibility of the mutants above was in fact due to the lack of the respective resistance modules, or whether those mutants exhibited a general growth defect that might result in increased bacitracin susceptibility. For instance, it is known that the BcrC phosphatase is also involved in Lipid II cycle progression under normal growth conditions (Bernard *et al.*, 2005), but the extent to which the cytosolic UPP phosphatase UppP (formerly YubB) could compensate for the deletion of BcrC was controversial (Cao and Helmann, 2002; Bernard *et al.*, 2005). To quantitatively test the fitness of the different mutants, we measured their doubling times in LB medium at 37 °C in a microplate reader (Fig. 2B). In the

absence of bacitracin, the wild type and $\Delta liaIH$ mutant grew at similar doubling times of $t_d = 23.0 \pm 2.2$ min, and $t_d = 24.7 \pm 2.1$ min, respectively, while the $\Delta bceAB$ mutant grew slightly faster ($t_d = 20.0 \pm 0.3$ min) and the $\Delta bcrC$ mutant significantly slower ($t_d = 28.7 \pm 1.7$ min) than wild type (P value of unpaired Student's *t*-test = 0.024). Moreover, we observed that under these conditions of rapid growth, the $\Delta bcrC$ mutant was about as sensitive as the $\Delta bceAB$ mutant, which displayed killing at 10 $\mu\text{g/ml}$ bacitracin and higher (Fig. 2B). This suggests that at high growth rates the deletion of *bcrC* can only be partially compensated for by the activity of the second UPP phosphatase UppP,, implying that UPP dephosphorylation might become the bottleneck for cell wall biosynthesis and hence for cell growth. Thus, we conclude that the increased bacitracin sensitivity of the $\Delta bcrC$ mutant can – at least partially – be attributed to a general growth defect incurred by reduced rates of UPP dephosphorylation.

Regulatory interactions between the CESR modules

The redundant contributions of the CESR modules to bacitracin resistance described above provoked the question of the extent to which deletion of one resistance module would affect the expression of the other resistance modules. To study these regulatory interactions, we fused the target promoter of each module to the *luxABCDE* cassette derived from *Photorhabdus luminescens* (Schmalisch *et al.*, 2010; Radeck *et al.*, 2013) and integrated the resulting reporter plasmids into the chromosome of wild type and mutants deficient in one of the three resistance modules (Table S1). Subsequently, exponentially growing cultures ($\text{OD}_{600} \approx 0.1$) were challenged with different bacitracin concentrations and the dose-dependent luciferase activity (one hour post-addition) was recorded as a proxy for promoter activity (Fig. 3).

Quantitative behavior of the unperturbed CESR network. In the wild type strain (Fig. 3, *black data*), P_{bceA} (Fig. 3A) displayed low activity (10^4 RLU/OD) in the absence of bacitracin and responded already at low bacitracin concentrations of $\geq 0.01 \mu\text{g ml}^{-1}$. This response gradually increased with rising bacitracin levels and reached its maximum about 300-fold over background at $30 \mu\text{g ml}^{-1}$ bacitracin. Recently, we showed that this gradual response over a high input-dynamic range is the result of negative feedback regulation in the Bce system, in which a flux-sensing mechanism homeostatically adjusts the rate of *de novo* transporter synthesis to the level needed for cell protection (Fritz *et al.*, 2015). In contrast to P_{bceA} , P_{bcrC} (Fig. 3B) already had a high basal activity (7×10^5 RLU/OD) and only responded at much higher bacitracin concentrations ($1 \mu\text{g ml}^{-1}$) with a maximum 3-fold induction over background at $30 \mu\text{g ml}^{-1}$. The strong P_{bcrC} activity in the absence of antibiotic treatment is consistent with the notion that BcrC is an important player in lipid II cycle progression under exponential growth conditions, as noted

above. Similar to P_{bceA} , P_{lial} (Fig. 3C) displayed a low basal activity and a strong (400-fold) induction at high bacitracin levels, but its input-dynamic range was much narrower (0.1 to 10 $\mu\text{g ml}^{-1}$ bacitracin) than seen for P_{bceA} (0.01 to 30 $\mu\text{g ml}^{-1}$ bacitracin). Hence, production of the primary resistance determinant BceAB is induced already at lower antibiotic concentrations than expression of the secondary resistance modules. This suggests that the primary layer might “buffer” against cell envelope stress at low bacitracin levels, while the demand for further protective measures only occurs at higher antibiotic concentrations.

BceAB is the pacemaker of the CESR network. If this buffering hypothesis was accurate, the secondary layer should become more sensitive and also more active in the absence of the primary resistance. Indeed, we found that in a $\Delta bceAB$ mutant the P_{bcrC} and P_{lialH} promoters were activated already at lower bacitracin concentrations and displayed a steeper dose-response behavior than in the wild type (Fig. 3B and C, *blue data*). Note that the activity of P_{bceA} itself remained at a basal level in the $\Delta bceAB$ mutant (Fig. 3A), again highlighting that the transport activity of BceAB is strictly required for activation of the P_{bceA} promoter (Rietkötter *et al.*, 2008; Fritz *et al.*, 2015). To further corroborate the buffering hypothesis, we next tested the effect of different constitutive BceAB levels on the expression of the secondary resistance layer. To this end, we complemented the $\Delta bceAB$ mutant with a xylose-inducible copy of *bceAB*. Strikingly, compared to the highly sensitive P_{lial} response in the $\Delta bceAB$ mutant (Fig. 4A (ii); *red data*), constitutive expression of *bceAB* at low levels was already sufficient to shift the induction threshold of the P_{lial} promoter to 3-fold higher bacitracin levels (Fig. 4A (ii); *orange data*). A high constitutive expression level of *bceAB* resulted in a further 10-fold increase of the P_{lial} induction threshold (Fig. 4A (ii); *light green data*), which could be even further increased by overexpression of *bceAB* in the wild type (Fig. 4A (ii); *dark green data*). Importantly, varying the *bceAB* expression level caused similar shifts in the induction threshold of the P_{bcrC} promoter (Fig. S1). Hence these data show that whenever the production level of BceAB is high, the expression of the two secondary resistance modules is low and *vice versa*. These clear-cut anti-correlations suggest that the ABC transporter actively prevents cell envelope stress and thereby reduces the demand for expression of the secondary layers of the CESR network.

Note that the variation of the *bceAB* expression levels also triggered shifts in the response of the P_{bceA} promoter itself (Fig. 4A (i)). Previously, we showed that this behavior can be rationalized by a flux-sensing mechanism, in which a sensory complex between the ABC transporter BceAB and the histidine kinase BceS detects the rate of bacitracin flux by individual transporters, which in turn activates the P_{bceA} promoter via the response regulator BceR (Fritz *et al.*, 2015). Accordingly, in cells with low BceAB levels the load per transporter saturates already

at low bacitracin levels and triggers full induction of P_{bceA} (Fig. 4A (i); *orange curve*). Conversely, in cells with higher BceAB levels the load per transporter saturates at significantly higher bacitracin levels, which in turn leads to proportional shifts of the P_{bceA} dose-response characteristic to the right (Fig. 4A (i); *green curves*) (Fritz *et al.*, 2015).

BcrC has pleiotropic effects on CESR modules. The deletion of *bcrC* triggered a 2- to 3-fold increased activity of its own promoter, P_{bcrC} , compared to the wild type (Fig. 3B, *green data*) – even in the absence of bacitracin stress. Given that the deletion of *bcrC* slowed down growth by impairing cell wall biosynthesis (Fig. 2B), the elevated P_{bcrC} activity seemed reasonable, because this promoter belongs to the regulon of the alternative sigma factor σ^M (Cao and Helmann, 2002). σ^M itself responds to a broad spectrum of cell envelope-perturbing agents (Eiamphungporn and Helmann, 2008) and was therefore considered to be a sensor for cell wall integrity (Inoue *et al.*, 2013; Lee and Helmann, 2013). Likewise, the P_{liaI} promoter activity was elevated 3-fold in the $\Delta bcrC$ mutant (Fig. 3C), consistent with the role of the Lia system as a general sensor of cell envelope stress (Wolf *et al.*, 2012). However, it was surprising that the P_{bceA} promoter was also up-regulated 10-fold in the $\Delta bcrC$ mutant (Fig. 3A), since previous reports were consistent with a model in which the Bce system responds to the detoxification flux of the *drug* and not to downstream *damage* on cell physiology (cf. Fig. 1C). This curious effect is discussed in more detail below.

To further substantiate that the observed phenotypes specifically arose from the deletion of *bcrC*, we complemented the $\Delta bcrC$ mutant with a xylose-inducible copy of *bcrC*. This complementation indeed returned the elevated activities of P_{bceA} and P_{liaI} back to wild-type levels (Fig. 4B; *light green data*). Interestingly, the overexpression of *bcrC* in a wild type background lead to a further decrease of both the P_{liaI} and P_{bceA} activities (Fig. 4B; *dark green data*), suggesting that an elevated rate of UPP dephosphorylation reduced the cellular susceptibility to bacitracin. Taken together, these data show that the level of BcrC sets the rate of UPP dephosphorylation, which in turn determines how many UPP target molecules the cell displays for binding by bacitracin. Accordingly, low levels of BcrC lead to the accumulation of UPP and make cells vulnerable to bacitracin attack, whereas high BcrC levels keep UPP levels low and make cells more resistant. This pattern is reflected both in the responses of the Lia and BcrC systems, which measure bacitracin-dependent damage of the cell envelope, as well as in the response of the Bce system, which presumably senses the UPP-bound form of bacitracin (see Discussion for more details).

LialH plays a positive autoregulatory role. In contrast to the marked effects the deletions of *bceAB* and *bcrC* had on the expression of all resistance modules, the deletion of *lialH* (Fig. 3, *orange data*) did not significantly influence the regulation of P_{bceA} and P_{bcrC} (Fig. 3A and B). However, the $\Delta lialH$ mutant displayed up to 7-fold reduced activity of its own promoter (Fig. 3C). This is the first report showing that the expression of the *lia* operon is not only regulated via the LiaFSR three-component system (Schrecke *et al.*, 2013), but that also the target proteins LialH play a positive autoregulatory role required for the full Lia response. In fact, when scrutinizing the temporal dynamics of promoter activities, it became evident that the $\Delta lialH$ mutant displayed only a transient P_{lial} induction that reached a peak between 10-20 min after bacitracin addition and declined afterwards, whereas the wild type displayed prolonged P_{lial} activity with a peak at ~40 min after bacitracin addition (Fig. S2).

In line with these observations, in a *lialH* complementation strain variations of the LialH production level did not affect the dose-response behavior of the P_{bceA} promoter, but had significant effects on P_{lial} activity itself (Fig. 4C). In the absence of bacitracin, the constitutive expression of *lialH* triggered a 20-fold increased P_{lial} activity compared to the wild type (Fig. 4C (ii); *light green data*). At bacitracin concentrations higher than 0.3 $\mu\text{g ml}^{-1}$, however, P_{lial} displayed a weaker activity than in wild type. These data show on the one hand that LialH has a positive regulatory effect on the P_{lial} promoter even in the absence of externally added antibiotics. On the other hand they show that the inability to up-regulate *lialH* lead to reduced P_{lial} activity, suggesting that a positive feedback via LialH might be needed for the full activation of the Lia system in wild type. To rule out that the marker-less deletion of *lialH* had polar effects on the expression of the signaling system LiaFSR, we complemented the $\Delta lialH$ mutant with a copy of *lialH* under the control of its native promoter (P_{lial}), and found that wild type behavior of P_{lial} induction could be restored (data not shown). Moreover, the overproduction of LialH in a wild type background (Fig. 4C (ii); *dark green data*) lead to an elevated P_{lial} activity in the absence of bacitracin, while at high bacitracin levels the Lia system was as active as in the wild type. Taken together, these results show that LialH has no influence on the primary resistance BceAB, but is instead involved in fully activating and perpetuating its own expression by a so far unknown mechanism. In the future, it remains to be clarified whether LialH is involved in the *perception* of cell envelope stress, or whether LialH *generates* some degree of envelope stress itself.

Single cell induction of CESR modules

The compensatory regulation between the different CESR modules observed at the bulk-level (see above), raises the question of how the bacterial population implements this response at the individual cell level. Do all cells within the population behave uniformly, or is there significant

phenotypic heterogeneity within the population? Given that the excess expression of resistance determinants is often associated with a fitness cost (Andersson and Hughes, 2010), it is in fact intriguing to ask whether bacteria evolved to *minimize* 'noise' in resistance gene expression (adjusting resistance as close as possible to its optimal level), or whether they actively *use* heterogeneous gene expression as a means to diversify resistance levels within the population – a strategy that can be beneficial in fluctuating environments (Fraser and Kaern, 2009).

To scrutinize the expression behavior of the three CESR modules at the single cell level, we fused their promoters to a plasmid-borne copy of *gfp* and introduced them into wild type *B. subtilis* W168. We then challenged exponentially growing cells with various levels of bacitracin and quantified GFP fluorescence by flow cytometry one hour after bacitracin addition (Fig. 5). In the absence of bacitracin the fluorescence distributions of the P_{bceA} -*gfp* (Fig. 5A) and the P_{lial} -*gfp* (Fig. 5C) reporters were identical to the autofluorescence distribution of *B. subtilis* W168 (data not shown), while the P_{bcrC} -*gfp* reporter activity was ~5-fold higher than background (Fig. 5B), consistent with the high basal activity of the P_{bcrC} promoter quantified with the luciferase reporter above (cf. Fig. 3). This suggests that the *gfp* reporter is less sensitive than the luciferase reporter, such that promoter activities below $\sim 10^5$ RLU/OD in Fig. 3 are hidden by the autofluorescence of *B. subtilis*. However, apart from this difference in reporter sensitivity, the mean fluorescence values for all promoter-*gfp* fusions were consistent with the results obtained for the promoter-*lux* fusions in Fig. 3.

Next, we compared gene expression noise in the response of the three resistance modules. As mentioned before, in the absence of bacitracin the fluorescence distributions of P_{bceA} -*gfp* (Fig. 5A) and P_{lial} -*gfp* (Fig. 5C) reporters were identical to the broad autofluorescence distribution of *B. subtilis*. In contrast, P_{bcrC} -*gfp* reporter displayed a narrow fluorescence distribution, and also showed low noise levels at all bacitracin levels tested. In the presence of bacitracin the response of the P_{bceA} -*gfp* reporter became almost as homogeneous as the P_{bcrC} -*gfp* reporter. Only the P_{lial} -*gfp* reporter was expressed broadly heterogeneously across the population when challenged with intermediate concentrations ($1-3 \mu\text{g ml}^{-1}$) of bacitracin (Fig. 5C), as reported before (Kesel *et al.*, 2013). Indeed, when quantifying gene expression noise by the coefficient of variation η , we found that at similar mean GFP expression levels the P_{lial} promoter was significantly noisier than the other promoters (Fig. S3A). This broadly heterogeneous production of LiaH argues for significant cell-to-cell variability in the downstream damage perceived by the Lia system in the presence of bacitracin. In contrast, the low noise levels in the expression of *bceAB* and *bcrC* suggest that their expression is subject to a more stringent control, which might be result of negative feedback regulation within these systems (see Discussion).

To test whether the noisy Lia response is influenced by the expression of the other two resistance modules, we introduced the $P_{liaI}-gfp$ reporter plasmid into $\Delta bceAB$ and $\Delta bcrC$ mutants and determined their single cell response towards bacitracin as above. Strikingly, the Lia response displayed notably less cell-to-cell variability in the $\Delta bceAB$ mutant than in the wild type (Fig. 5D). Also, when comparing their coefficients of variation at similar mean expression levels (Fig. S3B), we found that P_{liaI} is less noisy in the $\Delta bceAB$ mutant than in the wild type, thereby showing that the reduced noise level is not only caused by the stronger and more sensitive P_{liaI} response in this mutant. This suggests that in the unperturbed (wild type) CESR network, the broadly heterogeneous Lia response is directly triggered by heterogeneity in *bceAB* expression: At the time of antibiotic treatment there exists a narrow, yet stochastic distribution of BceAB protein levels across the population, such that cells with higher levels of BceAB have sufficient ability to cope with bacitracin, whereas cells with lower levels of BceAB experience more cell envelope damage, which in turn triggers higher LiaH production levels. Consequently, in the absence of BceAB this model predicts that all cells in the population would experience a similar envelope stress level, consistent with the homogeneous Lia response in the $\Delta bceAB$ mutant.

In contrast, our data showed that in a $\Delta bcrC$ mutant noise in the Lia response was markedly increased (Fig. 5D). We suggest that the increased noise in the expression of *bceAB* in this mutant (Fig. S4) leads to a significant heterogeneity in the downstream damage perceived by the Lia system. However, we cannot exclude that population heterogeneity in other lipid II cycle-associated players factors into the noise properties of P_{liaI} in this highly impaired mutant strain. For instance, stochastic expression of *uppP*, encoding the second, BacA-like UPP phosphatase in *B. subtilis* (Cao and Helmann, 2002; Bernard *et al.*, 2005; Inaoka and Ochi, 2012), could result in largely variable rates of cell wall biogenesis, which would in turn lead to phenotypic heterogeneity in the susceptibility towards cell wall antibiotics.

Discussion

After the discovery of the bacitracin stimulon in *Bacillus subtilis* (Mascher *et al.*, 2003) and the quantitative characterization of its individual modules (Rietkötter *et al.*, 2008), we here present the first description of the full anatomy of the bacitracin resistance network in *B. subtilis*. Using a systems-level approach we showed that a clear hierarchy exists between resistance modules, allowing us to discriminate between primary (BceAB) and secondary layers (BcrC and LiaH) of bacitracin resistance. Strikingly, in mutants devoid of the primary resistance layer, the secondary layer was more strongly induced, revealing a high level of redundancy between resistance modules. Accordingly, our data now show for the first time that in the absence of the primary bacitracin resistance module, the deletion of *liaIH* displays a clear-cut phenotype with a 6-fold

reduction of bacitracin resistance. Hence, we argue that the high level of resistance conferred by BceAB masks the weaker contribution from the Lia system. This explains previous reports that noted surprisingly weak phenotypes of a *liaIH* deletion alone, despite the strong Lia expression under a variety of cell envelope-perturbing conditions, including lipid II cycle-interfering antibiotics as well as oxidative stress reagents (Jordan *et al.*, 2006; Rietkötter *et al.*, 2008; Suntharalingam *et al.*, 2009; Wolf *et al.*, 2010). So far, one of the strongest phenotypes was found during treatment with the membrane pore-forming lipopeptide daptomycin, where a *liaIH* deletion caused a 3-fold reduction of resistance (Hachmann *et al.*, 2009; Wecke *et al.*, 2009). Notably, *B. subtilis* features no primary resistance mechanism against daptomycin, again highlighting that the contribution of the Lia system to antibiotic resistance is strongest if other resistance layers are lacking. Based on these observations, and in conjunction with the wide distribution of the PspA/IM30 protein family (of which LiaH is a member) across various bacterial phyla and even in archaea and eukaryotes (Joly *et al.*, 2010), we speculate that the Lia system constitutes an ancient resistance module that provides a low level of resistance against a broad range of cell envelope-perturbing agents. In contrast, the Bce-like resistance modules confer high levels of protection against a rather narrow range of antimicrobial peptides (Gebhard, 2012) and are almost exclusively found in Firmicutes bacteria (Joseph *et al.*, 2002; Mascher, 2006; Dintner *et al.*, 2011), suggesting that these specialized resistance layers were acquired later during evolution.

The results presented here also shed new light on the role of the UPP phosphatase BcrC in lipid II cycle homeostasis under antimicrobial peptide attack. First, we showed that the deletion of *bcrC* lead to a significant decrease in growth rate - even in the absence of antibiotic treatment. It appears likely that the second BacA-like UPP phosphatase, UppP, partially compensates for the loss of BcrC, but that its activity is insufficient to maintain adequate cell wall synthesis under the rapid growth conditions in LB media. The precise extent to which the *uppP* promoter is up-regulated in such a mutant, and how it responds to lipid II cycle-inhibiting antimicrobial peptides, remains to be elucidated. Second, our data revealed that *bcrC* deletion had pleiotropic effects on the expression of all resistance modules and, most notably, triggered their up-regulation also in the absence of externally added bacitracin. In these highly perturbed cells, the induction of the Lia system was consistent with its role as a general sensor of cell envelope stress (Wolf *et al.*, 2010). Likewise, the up-regulation of the σ^M - and σ^X -dependent P_{bcrC} promoter was not unexpected, because these alternative σ factors were also shown to be sensors for cell wall integrity (Inoue *et al.*, 2013; Lee and Helmann, 2013). However, it was surprising to find the P_{bceA} promoter affected in the *bcrC* mutant, because all previous reports

were consistent with a model in which the Bce system responds to the detoxification flux of the drug and not to downstream damage on cell physiology (Wolf *et al.*, 2012; Fritz *et al.*, 2015).

One possible explanation for the elevated P_{bceA} activity might be that the lack of the phosphatase BcrC causes the accumulation of UPP in the membrane, and thereby provides a surplus of targets for bacitracin. In turn, increased levels of UPP-bacitracin complexes would increase the detoxification flux per BceAB transporter, which then serves as the signal for P_{bceA} activation. While this model can explain the increased P_{bceA} activity in the presence of bacitracin, it is less intuitive why there was also a ~10-fold activation in the absence of bacitracin (cf. Fig. 3A). One possibility is that the accumulation of UPP itself somehow triggers BceAB activity. Interestingly, Kingston and colleagues suggested that BceAB may recognize UPP directly and flip it to the inner face of the membrane, where it may be protected from bacitracin and dephosphorylated by a cytosolically acting UppP (Kingston *et al.*, 2014). Although it is known that BceB directly binds free bacitracin *in vitro* with high affinity (Dintner *et al.*, 2014), it is conceivable that the physiological substrate of the transporter is the UPP-bacitracin complex in the cell, as suggested previously (Fritz *et al.*, 2015). In this case, the transporter may also be able to interact with both components of the complex separately, i.e., free bacitracin and free UPP, especially when increased amounts of these are present. The increased basal activity of P_{bceA} in the *bcrC* mutant may then be due to accumulation of UPP. A third alternative explanation might be that one or more of the endogeneously produced antimicrobial peptides activate the Bce system under these conditions. For instance, we recently showed that the endogenous production of the sporulation delay protein C (SdpC) and the sporulation killing factor A (SkfA) in early stationary phase up-regulate production of BceAB and the paralogous PsdAB transporter in *B. subtilis* more than 100-fold (Höfler *et al.*, 2016).

Taken together, the work from us and earlier work support the following, multi-layered model of the bacitracin resistance network in *B. subtilis*: In the presence of bacitracin (Bac) the accumulation of UPP-bacitracin (UPP-Bac) complexes blocks the lipid II cycle of cell wall biosynthesis and, as a consequence, leads to cell envelope damage. UPP-Bac is recognized by the ABC transporter BceAB, which releases UPP from the inhibitory grip of bacitracin by a so far unknown transport mechanism and thereby shifts the binding equilibrium towards the free form of UPP. Expression of *bceAB* is controlled by a flux-sensing mechanism (Fig. 1C), which homeostatically adjusts the BceAB level such that the transport activity of individual ABC transporters does not exceed a critical threshold (Fritz *et al.*, 2015). At the same time such homeostatic, negative feedback systems are known to reduce gene expression noise (Alon, 2007), fully consistent with the homogeneous response of the Bce system observed at the single cell level. Simultaneously to the action of BceAB, BcrC reduces the concentration of the

415 bacitracin-target UPP by dephosphorylation to UP, thereby further promoting progression of the
416 lipid II cycle. Under bacitracin stress, transcription of *bcrC* is controlled by the alternative ECF σ
417 factor σ^M , which is regulated by the membrane-bound anti- σ factors YhdK/L (Fig. 1C). Previous
418 data showed that either the depletion of UP and/or the depletion of lipid II could be the cues for
419 anti- σ factors YhdK/L (Inoue *et al.*, 2013; Lee and Helmann, 2013; Meeske *et al.*, 2015). This
420 suggests that the end product of the reaction catalyzed by BcrC (UPP \rightarrow UP) could negatively
421 regulate the expression of *bcrC*, which would in turn close a negative feedback loop that asserts
422 homeostatic UP level control in the cell. This model is also consistent with all our data, most
423 importantly the elevated P_{bcrC} activity in the *bcrC* mutant (which we expect to display low UP
424 levels), as well as the low noise level of the P_{bcrC} promoter, which is again characteristic of
425 negative feedback systems. Within our model, the Lia system constitutes the last line of defense
426 that directly responds to and combats cell envelope damage, thereby explaining why the
427 expression of the Lia system did not affect the expression of the other resistance modules in our
428 data.

429 More generally, we propose that the redundant organization of the bacitracin resistance
430 network of *B. subtilis* described here is a universal principle of many stress response networks
431 within the microbial world, as demonstrated for instance in the oxidative stress responses of
432 *Salmonella enterica* (Hébrard *et al.*, 2009) and *Ralstonia solanacearum* (Flores-Cruz and Allen,
433 2009) or in the regulation of drug efflux systems in various bacterial species (Grkovic *et al.*,
434 2002). Here the induction of individual stress response modules typically relieves stress
435 perceived by other modules, which can be interpreted as a coupling between stress response
436 modules via a global negative feedback mechanism. Failure of one of the 'nodes' in such a
437 network then triggers compensatory up-regulation of other nodes, which then jointly protect the
438 cell. Interestingly, in the engineering disciplines this concept is known as 'active redundancy',
439 during which the performance of individual devices is automatically monitored and dynamically
440 reconfigured to eliminate performance declines of the system (Pahl and Beitz, 1996). In contrast,
441 'passive redundancy' uses excess capacity to reduce the impact of component failures (Pahl
442 and Beitz, 1996), which would be akin to the constitutive expression of all resistance
443 determinants. In biological stress response networks, we propose that the use of active
444 redundancy serves as an optimal regulation strategy to maximize cellular protection while
445 preventing the direct or indirect costs of excess resistance gene expression.

447 **Acknowledgements**

448 This project was funded by the DFG priority program SPP1617 'Phenotypic Heterogeneity and
449 Sociobiology of Bacterial Populations' (grants FR 3673/1-2 to GF and MA 2837/3-2 to TM).

Materials and Methods

Bacterial strains and growth conditions

Bacillus subtilis and *Escherichia coli* were routinely grown in Luria-Bertani (LB) medium at 37°C with agitation (200 rpm). Transformations of *B. subtilis* were carried out as described previously (Harwood and Cutting, 1990). All strains used in this study are derivatives of the wild-type strain W168 and are listed in Table S1. Kanamycin (10 mg ml⁻¹), chloramphenicol (5 mg ml⁻¹), spectinomycin (100 mg ml⁻¹), tetracycline (10 mg ml⁻¹) and erythromycin (1 mg ml⁻¹) plus lincomycin (25 mg ml⁻¹) for macrolide-lincosamide-streptogramin B ('MLS') resistance were used for the selection of the *B. subtilis* mutants used in this study. Solid media contained 1.5% (w/v) agar. For complementation studies, full induction of the promoter P_{xyIA} was achieved by adding xylose to a final concentration of 0.2 % (w/v).

DNA manipulation

Plasmids were generated by using standard cloning techniques (Sambrook, Russell 2001) with enzymes and buffers from New England Biolabs (NEB; Ipswich, MA, USA) according to the respective protocols. PCR-DNA amplification for cloning purposes occurred with Phusion® or Q5® polymerase. Primers used in this study are listed in Table S2 and plasmid descriptions as well as details on their construction are given in Table S3. All plasmids were verified by sequencing of the insert. The integration of plasmids or DNA fragments into the genome, or the presence of a replicative vector, was confirmed by colony PCR. Integration into the *thrC*-locus was checked by threonine-auxotrophy in minimal medium.

Determination of minimal inhibitory concentration

Bacitracin resistance of *B. subtilis* strains was determined using Etest® strips on bacterial lawn (bioMérieux, Marcy l'Etoile, France), providing a concentration range from 256 to 0.016 µg ml⁻¹ bacitracin. Briefly, 3 ml of Müller-Hinton (MH) medium (2.1% (w/v) Müller-Hinton broth) were inoculated 1:100 from fresh overnight culture and cells were grown at 37°C with agitation to OD₆₀₀ = 0.6-0.8. Subsequently, 30 µl of the cell suspension were added to 3 ml molten MH soft agar (60°C, 0.75% (w/v) agar), mixed and distributed on MH agar plates. After 20 min of solidification, one Etest® strip was applied per agar plate. Results were documented after 24 h of incubation at 37°C.

Luciferase assays

Luciferase activities of *B. subtilis* strains harboring pBS3*Clux*-derivates were assayed using a SynergyTM NEOALPHAB multi-mode microplate reader from BioTek[®] (Winooski, VT, USA). The reader was controlled using the software Gen5TM (version 2.06). Cells were inoculated 1:1000 from fresh overnight cultures and grown to OD₆₀₀ = 0.1-0.5. Subsequently, cultures were diluted to OD₆₀₀ = 0.01 and split into 100 µl per well in 96-well plates (black walls, clear bottom; Greiner Bio-One, Frickenhausen, Germany). Cultures were incubated at 37°C with linear agitation (intensity, 567 cpm) and the optical density at 600 nm (OD₆₀₀) as well as luminescence was monitored every 5 min. After one hour, freshly diluted Zn²⁺-bacitracin was added to the indicated final concentrations and incubation and monitoring was resumed for 2 hours. Specific luminescence activity is given by the raw luminescence output (relative luminescence units, RLU) normalized by cell density (RLU/OD).

Flow cytometry assays

Single-cell fluorescence of *B. subtilis* strains carrying GFP-reporter plasmids was measured using a BD AccuriTM C6 flow cytometer (BD Biosciences, Becton, Dickinson and Company, New Jersey, USA). Cells were inoculated 1:1000 from overnight cultures and grown at 37°C to OD₆₀₀~0.1. Subsequently the culture was split into test tubes, stained with FM[®] 4-64 (Life Technologies GmbH, USA) to a final concentration of 2 ng ml⁻¹ and incubated at 37°C with agitation. After 30 min cells were induced with indicated final concentrations of Zn²⁺-bacitracin and 1 hour after further incubation, culture samples were assayed by flow cytometry. It was controlled by the BD AccuriTM C6 software using the following settings: sample threshold = 11,000 on FSC-H, core size = 5µm, flow rate = 10 µl min⁻¹. Noise in the resulting fluorescence distributions (cf. Fig. S3) was quantified by the coefficient of variation η , defined as the ratio of the standard deviation σ to the mean μ . In doing so, we used the geometric mean and variance, because those measures are known to yield more accurate statistics for log-normal distributed values than the arithmetic mean and standard deviation.

References

- Alon, U. (2007) Network motifs: theory and experimental approaches. *Nat Rev Genet* **8**: 450–461.
- Andersson, D.I., Hughes, D. (2010) Antibiotic resistance and its cost: is it possible to reverse resistance? *Nat Rev Microbiol* **8**: 260–271.
- Aso, Y., Okuda, K.-I., Nagao, J.-I., Kanemasa, Y., Thi Bich Phuong, N., Koga, H., *et al.* (2005) A novel type of immunity protein, NukH, for the lantibiotic nukacin ISK-1 produced by *Staphylococcus warneri* ISK-1. *Biosci Biotechnol Biochem* **69**: 1403–1410.
- Azevedo, E.C., Rios, E.M., Fukushima, K., and Campos-Takaki, G.M. (1993) Bacitracin production by a new strain of *Bacillus subtilis*. *Appl Biochem Biotechnol* **42**: 1–7.
- Bernard, R., Ghachi, El, M., Mengin-Lecreulx, D., Chippaux, M., and Denizot, F. (2005) BcrC from *Bacillus subtilis* acts as an undecaprenyl pyrophosphate phosphatase in bacitracin resistance. *J Biol Chem* **280**: 28852–28857.
- Breukink, E., and de Kruijff, B. (2006) Lipid II as a target for antibiotics. *Nat Rev Drug Discov* **5**: 321–332.
- Cao, M., and Helmann, J.D. (2002) Regulation of the *Bacillus subtilis* *bcrC* bacitracin resistance gene by two extracytoplasmic function sigma factors. *J Bacteriol* **184**: 6123–6129.
- Dintner, S., Heermann, R., Fang, C., Jung, K., and Gebhard, S. (2014) A sensory complex consisting of an ATP-binding cassette transporter and a two-component regulatory system controls bacitracin resistance in *Bacillus subtilis*. *J Biol Chem* **289**: 27899–27910.
- Dintner, S., Staroń, A., Berchtold, E., Petri, T., Mascher, T., and Gebhard, S. (2011) Coevolution of ABC transporters and two-component regulatory systems as resistance modules against antimicrobial peptides in Firmicutes bacteria. *J Bacteriol* **193**: 3851–3862.
- Domínguez-Escobar, J., Wolf, D., Fritz, G., Höfler, C., Wedlich-Söldner, R., and Mascher, T. (2014) Subcellular localization, interactions and dynamics of the phage-shock protein-like Lia response in *Bacillus subtilis*. *Mol Microbiol* **92**: 716–732.
- Economou, N.J., Cocklin, S., and Loll, P.J. (2013) High-resolution crystal structure reveals molecular details of target recognition by bacitracin. *P Natl Acad Sci USA* **110**: 14207–14212.
- Eiamphungporn, W., and Helmann, J.D. (2008) The *Bacillus subtilis* σ^M regulon and its contribution to cell envelope stress responses. *Mol Microbiol* **67**: 830–848.
- Eijsink, V.G.H., Axelsson, L., Diep, D.B., Håvarstein, L.S., Holo, H., and Nes, I.F. (2002) Production of class II bacteriocins by lactic acid bacteria; an example of biological warfare and communication. *Antonie Van Leeuwenhoek* **81**: 639–654.
- Flores-Cruz, Z., Allen, C. (2009) *Ralstonia solanacearum* encounters an oxidative environment during tomato infection. *Mol Plant Microbe Interact* **22**: 773–782.
- Fraser, D., Kaern, M. (2009) A chance at survival: gene expression noise and phenotypic diversification strategies. *Mol Microbiol* **71**: 1333–1340.

547 Fritz, G., Dintner, S., Treichel, N.S., Radeck, J., Gerland, U., Mascher, T., and Gebhard, S.
548 (2015) A new way of sensing: Need-based activation of antibiotic resistance by a flux-sensing
549 mechanism. *mBio* **6**: e00975.

550 Gebhard, S. (2012) ABC transporters of antimicrobial peptides in Firmicutes bacteria -
551 phylogeny, function and regulation. *Mol Microbiol* **86**: 1295–1317.

552 Grkovic, S., Brown, M.H., and Skurray, R.A. (2002) Regulation of bacterial drug export systems.
553 *Microbiol Mol Biol Rev* **66**: 671–701.

554 Hachmann, A.-B., Angert, E.R., and Helmann, J.D. (2009) Genetic analysis of factors affecting
555 susceptibility of *Bacillus subtilis* to daptomycin. *Antimicrob Agents Chemother* **53**: 1598–1609.

556 Hébrard, M., Viala, J.P.M., Méresse, S., Barras, F., Aussel, L. (2009) Redundant hydrogen
557 peroxide scavengers contribute to *Salmonella* virulence and oxidative stress resistance. *J*
558 *Bacteriol* **191**: 4605–4614.

559 Höfler, C., Heckmann, J., Fritsch, A., Popp, P., Gebhard, S., Fritz, G., and Mascher, T. (2016)
560 Cannibalism Stress Response in *Bacillus subtilis*. *Microbiology* [Epub ahead of print; doi:
561 10.1099/mic.0.000176].

562 Inaoka, T., and Ochi, K. (2012) Undecaprenyl Pyrophosphate involvement in susceptibility of
563 *Bacillus subtilis* to rare earth elements. *J Bacteriol* **194**: 5632–5637.

564 Inoue, H., Suzuki, D., and Asai, K. (2013) A putative bactoprenol glycosyltransferase, CsbB, in
565 *Bacillus subtilis* activates SigM in the absence of co-transcribed YfhO. *Biochem Biophys Res*
566 *Commun* **436**: 6–11.

567 Ishihara, H., Takoh, M., Nishibayashi, R., and Sato, A. (2002) Distribution and variation of
568 bacitracin synthetase gene sequences in laboratory stock strains of *Bacillus licheniformis*. *Curr*
569 *Microbiol* **45**: 18–23.

570 Joly, N., Engl, C., Jovanovic, G., Huvet, M., Toni, T., Sheng, X., *et al.* (2010) Managing
571 membrane stress: the phage shock protein (Psp) response, from molecular mechanisms to
572 physiology. *FEMS Microbiol Rev* **34**: 797–827.

573 Jordan, S., Junker, A., Helmann, J.D., and Mascher, T. (2006) Regulation of LiaRS-dependent
574 gene expression in *Bacillus subtilis*: identification of inhibitor proteins, regulator binding sites,
575 and target genes of a conserved cell envelope stress-sensing two-component system. *J*
576 *Bacteriol* **188**: 5153–5166.

577 Jordan, S., Rietkötter, E., Strauch, M.A., Kalamorz, F., Butcher, B.G., Helmann, J.D., and
578 Mascher, T. (2007) LiaRS-dependent gene expression is embedded in transition state regulation
579 in *Bacillus subtilis*. *Microbiology* **153**: 2530–2540.

580 Jordan, S., Hutchings, M.I., and Mascher, T. (2008) Cell envelope stress response in Gram-
581 positive bacteria. *FEMS Microbiol Rev* **32**: 107–146.

582 Joseph, P., Fichant, G., Quentin, Y., Denizot, F. (2002) Regulatory relationship of two-
583 component and ABC transport systems and clustering of their genes in the *Bacillus/Clostridium*
584 group, suggest a functional link between them. *J Mol Microbiol Biotechnol* **4**: 503–513.

585 Kesel, S., Mader, A., Höfler, C., Mascher, T., and Leisner, M. (2013) Immediate and

586 heterogeneous response of the LiaFSR two-component system of *Bacillus subtilis* to the peptide
587 antibiotic bacitracin. *PLoS ONE* **8**: e53457.

588 Kingston, A.W., Zhao, H., Cook, G.M., and Helmann, J.D. (2014) Accumulation of heptaprenyl
589 diphosphate sensitizes *Bacillus subtilis* to bacitracin: implications for the mechanism of
590 resistance mediated by the BceAB transporter. *Mol Microbiol* **93**: 37–49.

591 Kleerebezem, M., Crielaard, W., and Tommassen, J. (1996) Involvement of stress protein PspA
592 (phage shock protein A) of *Escherichia coli* in maintenance of the protonmotive force under
593 stress conditions. *EMBO J* **15**: 162–171.

594 Kobayashi, R., Suzuki, T., and Yoshida, M. (2007) *Escherichia coli* phage-shock protein A
595 (PspA) binds to membrane phospholipids and repairs proton leakage of the damaged
596 membranes. *Mol Microbiol* **66**: 100–109.

597 Lee, Y.H., and Helmann, J.D. (2013) Reducing the level of undecaprenyl pyrophosphate
598 synthase has complex effects on susceptibility to cell wall antibiotics. *Antimicrob Agents*
599 *Chemother* **57**:4267–4275.

600 Mascher, T., Margulis, N.G., Wang, T., Ye, R.W., and Helmann, J.D. (2003) Cell wall stress
601 responses in *Bacillus subtilis*: the regulatory network of the bacitracin stimulon. *Mol Microbiol* **50**:
602 1591–1604.

603 Mascher, T., Zimmer, S.L., Smith, T.-A., and Helmann, J.D. (2004) Antibiotic-inducible promoter
604 regulated by the cell envelope stress-sensing two-component system LiaRS of *Bacillus subtilis*.
605 *Antimicrob Agents Chemother* **48**: 2888–2896.

606 Mascher, T. (2006) Intramembrane-sensing histidine kinases: a new family of cell envelope
607 stress sensors in Firmicutes bacteria. *FEMS Microbiol Lett* **264**: 133–144.

608 Meeske, A.J., Sham, L.-T., Kimsey, H., Koo, B.-M., Gross, C.A., Bernhardt, T.G., and Rudner,
609 D.Z. (2015) MurJ and a novel lipid II flippase are required for cell wall biogenesis in *Bacillus*
610 *subtilis*. *P Natl Acad Sci USA* **112**: 6437–6442.

611 Ohki, R., Giyanto, Tateno, K., Masuyama, W., Moriya, S., Kobayashi, K., and Ogasawara, N.
612 (2003) The BceRS two-component regulatory system induces expression of the bacitracin
613 transporter, BceAB, in *Bacillus subtilis*. *Mol Microbiol* **49**: 1135–1144.

614 Pahl, G., and Beitz, W. (1996). *Engineering design*, Springer.

615 Radeck, J., Kraft, K., Bartels, J., Cikovic, T., Dürr, F., Emenegger, J., *et al.* (2013) The *Bacillus*
616 BioBrick Box: generation and evaluation of essential genetic building blocks for standardized
617 work with *Bacillus subtilis*. *J Biol Eng* **7**: 29.

618 Revilla-Guarinos, A., Gebhard, S., Mascher, T., and Zúñiga, M. (2014) Defence against
619 antimicrobial peptides: different strategies in Firmicutes. *Environ Microbiol.* **16**: 1225-1237.

620 Rietkötter, E., Hoyer, D., and Mascher, T. (2008) Bacitracin sensing in *Bacillus subtilis*. *Mol*
621 *Microbiol* **68**: 768–785.

622 Schmalisch, M., Maiques, E., Nikolov, L., Camp, A.H., Chevreux, B., Muffler, A., *et al.* (2010)
623 Small genes under sporulation control in the *Bacillus subtilis* genome. *J Bacteriol* **192**: 5402–
624 5412.

625 Schrecke, K., Jordan, S., and Mascher, T. (2013) Stoichiometry and perturbation studies of the
626 LiaFSR system of *Bacillus subtilis*. *Mol Microbiol* **87**: 769–788.

627 Schrecke, K., Staroń, A., Mascher, T. (2012) Two-component signalling in the Gram-positive
628 envelope stress response: Intramembrane-sensing histidine kinases and accessory membrane
629 proteins, p. 426. *In* Gross, R., Beier, D. (eds.), Two-component systems in bacteria. Horizon
630 Scientific Press.

631 Staroń, A., Finkeisen, D.E., and Mascher, T. (2011) Peptide antibiotic sensing and detoxification
632 modules of *Bacillus subtilis*. *Antimicrob Agents Chemother* **55**: 515–525.

633 Stein, T., Heinzmann, S., Solovieva, I., and Entian, K.-D. (2003) Function of *Lactococcus lactis*
634 nisin immunity genes *nisl* and *nisFEG* after coordinated expression in the surrogate host *Bacillus*
635 *subtilis*. *J Biol Chem* **278**: 89–94.

636 Storm, D.R., and Strominger, J.L. (1973) Complex formation between bacitracin peptides and
637 isoprenyl pyrophosphates. The specificity of lipid-peptide interactions. *J Biol Chem* **248**: 3940–
638 3945.

639 Suntharalingam, P., Senadheera, M.D., Mair, R.W., Lévesque, C.M., and Cvitkovitch, D.G.
640 (2009) The LiaFSR system regulates the cell envelope stress response in *Streptococcus mutans*.
641 *J Bacteriol* **191**: 2973–2984.

642 Wecke, T., Zühlke, D., Mäder, U., Jordan, S., Voigt, B., Pelzer, S., *et al.* (2009) Daptomycin
643 versus Friulimicin B: in-depth profiling of *Bacillus subtilis* cell envelope stress responses.
644 *Antimicrob Agents Chemother* **53**: 1619–1623.

645 Wolf, D., Domínguez-Cuevas, P., Daniel, R.A., and Mascher, T. (2012) Cell envelope stress
646 response in cell wall-deficient L-forms of *Bacillus subtilis*. *Antimicrob Agents Chemother* **56**:
647 5907–5915.

648 Wolf, D., Kalamorz, F., Wecke, T., Juszczak, A., Mäder, U., Homuth, G., *et al.* (2010) In-depth
649 profiling of the LiaR response of *Bacillus subtilis*. *J Bacteriol* **192**: 4680–4693.

650

651

652

653

654

655

656

Figure Legends

Figure 1. Schematic overview of bacitracin resistance determinants and their regulation

(A) In the absence of bacitracin, the membrane-associated steps of cell wall biosynthesis in *B. subtilis* involve the cytosolic attachment of peptidoglycan precursors to the lipid carrier undecaprenyl-phosphate (UP) via MraY and MurG, followed by transport of the resulting lipid II molecule to the extracytoplasmic leaflet of the cytoplasmic membrane via at least two redundant flippases MraY and Amj. After incorporating peptidoglycan precursors into the cell wall by penicillin binding proteins (PBPs), the remaining phosphorylated form of the lipid carrier, undecaprenyl-pyrophosphate (UPP), is converted to UP via the phosphatase BcrC, before it can enter the next transport cycle. Bacitracin blocks this essential lipid II cycle by tightly binding to UPP and thereby preventing the recycling of the lipid carrier. Bacitracin resistance is conferred by the increased production of the ABC-transporter BceAB, which removes bacitracin from UPP by a so far unknown transport mechanism, and the increased production of BcrC, which allows the lipid II cycle to progress in the presence of bacitracin. **(B)** The third player in the bacitracin stress response network is the phage-shock protein-like Lia response. Upon bacitracin challenge, the small membrane anchor Lial recruits the cytosolic PspA/IM30 protein family member LiaH into membrane-associated patches of unknown physiological function. Potentially, these structures stabilize the membrane underneath damaged areas of the cell wall. **(C)** Regulation scheme of the bacitracin stress response network in *B. subtilis*. Expression of *bceAB* is activated via a flux-sensing mechanism, monitoring the detoxification flux of the ABC transporter BceAB via complex formation between BceAB and the histidine kinase BceS (Dintner *et al.*, 2014; Fritz *et al.*, 2015), which in turn activates transcription via phosphorylation of the response regulator BceR. Expression of *bcrC* is regulated by the ECF σ -factors σ^M and σ^X and their cognate anti σ -factors, which together are considered to be sensors for cell wall integrity (Inoue *et al.*, 2013; Lee and Helmann, 2013). Likewise, expression of *liaIH* is regulated by the LiaFSR three-component system (Jordan *et al.*, 2006; Mascher, 2006; Schrecke *et al.*, 2013), which has also been shown to be a sensor of cell envelope damage (Wolf *et al.*, 2012).

Figure 2. Contributions of CESR modules to bacitracin resistance. (A) Minimal inhibitory concentration (MIC) of indicated *B. subtilis* strains as determined by the E-test[®] agar gradient diffusion method on Müller-Hinton medium. Strains tested were W168, TMB35 ($\Delta bceAB$), TMB297 ($\Delta bcrC$), TMB1151 ($\Delta liaIH$), TMB713 ($\Delta bceAB \Delta bcrC$), TMB2127 ($\Delta bceAB \Delta liaIH$), TMB2128 ($\Delta bcrC \Delta liaIH$) and TMB1829 ($\Delta bceAB \Delta bcrC \Delta liaIH$). Pictures are representative for three biological replicates with a maximal sample deviation of one concentration step; arrows

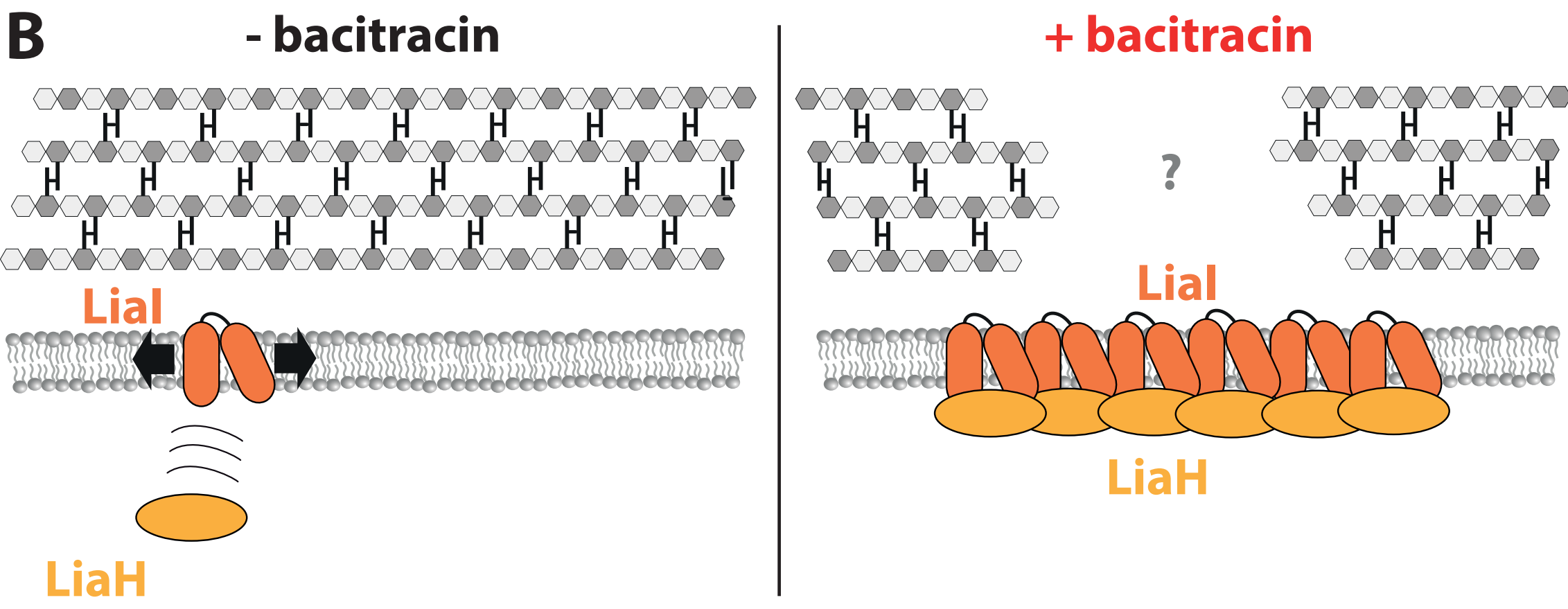
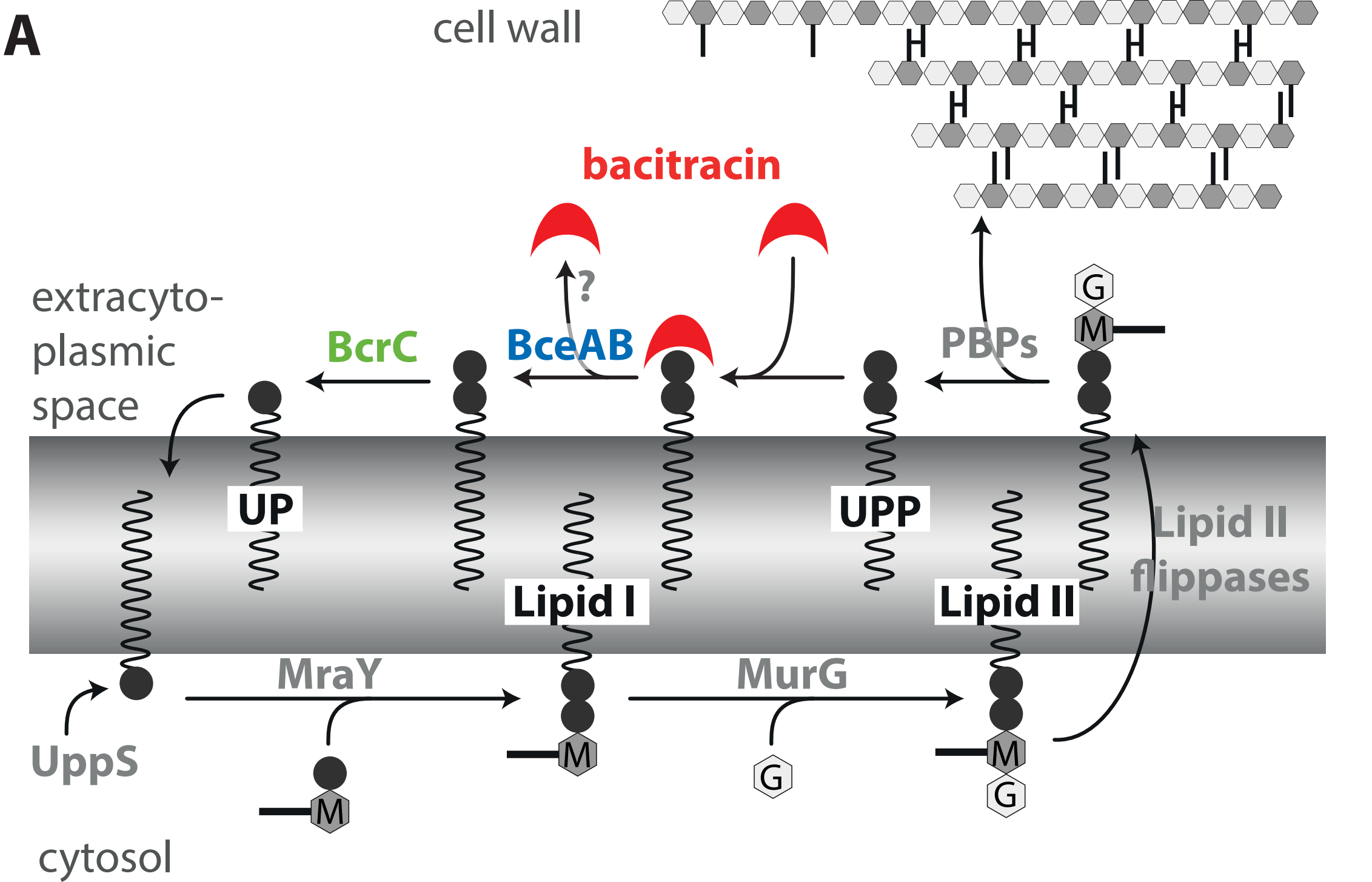
indicate the fold-change of sensitivity. **(B)** Doubling times of exponentially growing cells one hour after treatment with indicated bacitracin concentration. Graphs show data for single mutant strains containing the *lux*-reporter, see caption of figure 3. Standard deviation was obtained from at least nine biological replicates.

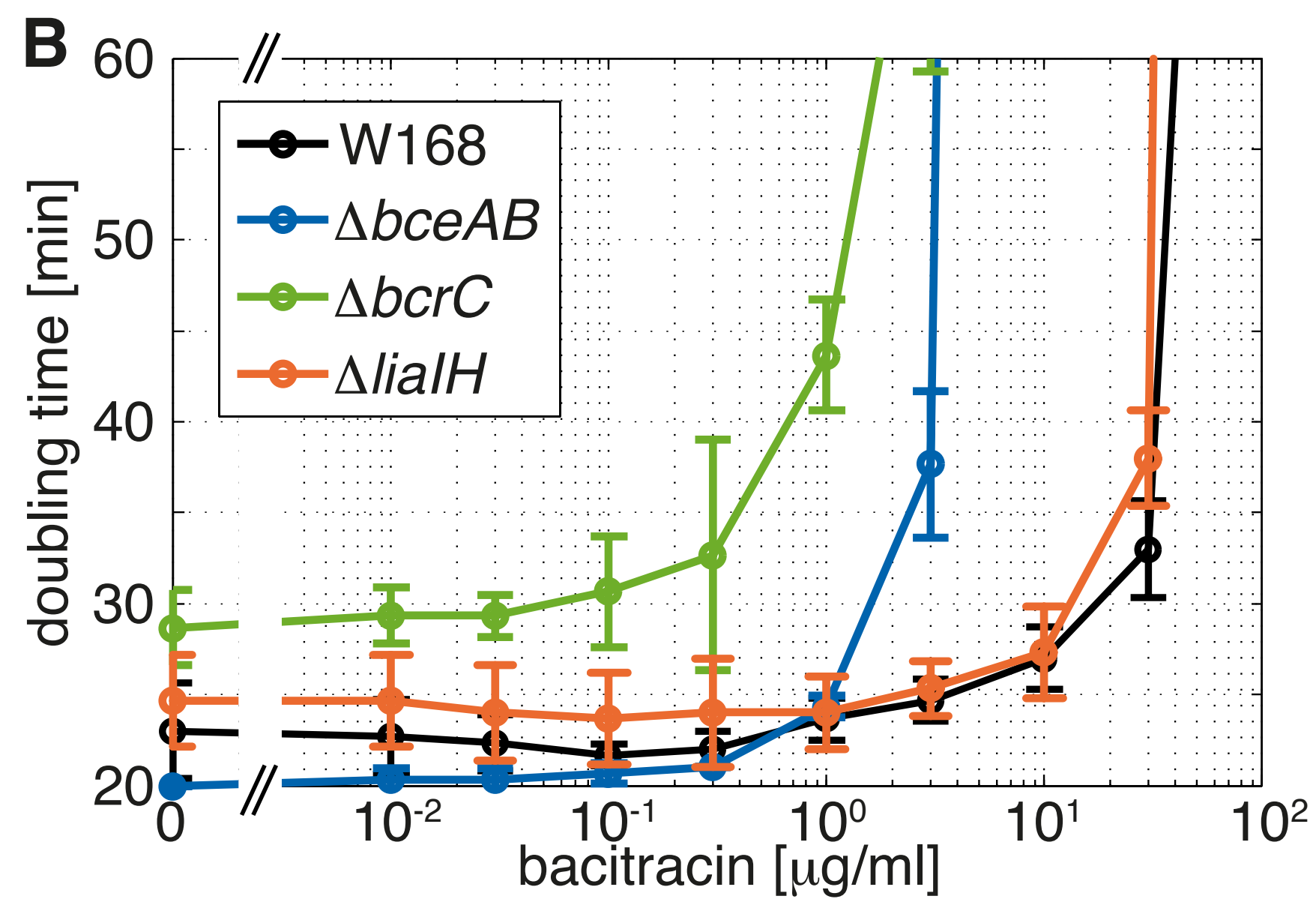
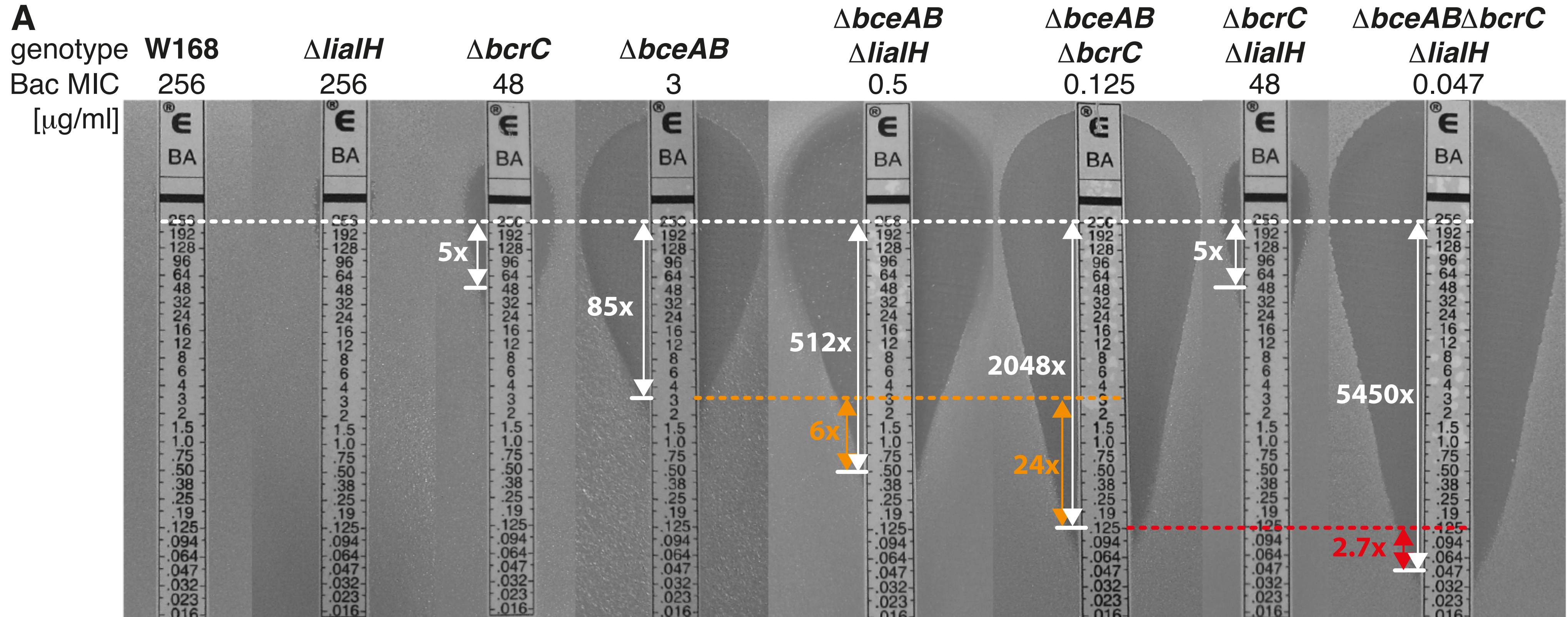
Figure 3. Dose-dependent activation of resistance modules in perturbed and unperturbed CESR networks. Target promoter activities of **(A)** P_{bceA} -*lux*, **(B)** P_{bcrC} -*lux* and **(C)** P_{lialH} -*lux* in strains carrying indicated deletions of CESR modules, as given by specific luciferase activity (RLU/OD₆₀₀) one hour after addition of indicated amounts of bacitracin. Measurements were performed during exponential growth phase in LB medium at 37°C in a microtiter plate reader. Data are shown for strains TMB1619, TMB1620, TMB1617 (W168); TMB1623, TMB1624, TMB1621 ($\Delta bceAB$); TMB1627, TMB1628, TMB1625 ($\Delta bcrC$) and TMB1661, TMB1662, TMB1659 ($\Delta lialH$) containing P_{bceA} -*lux*, P_{bcrC} -*lux* or P_{lialH} -*lux*, respectively, see Table S1. Data points and error bars indicate means and standard deviations derived from at least three biological replicates.

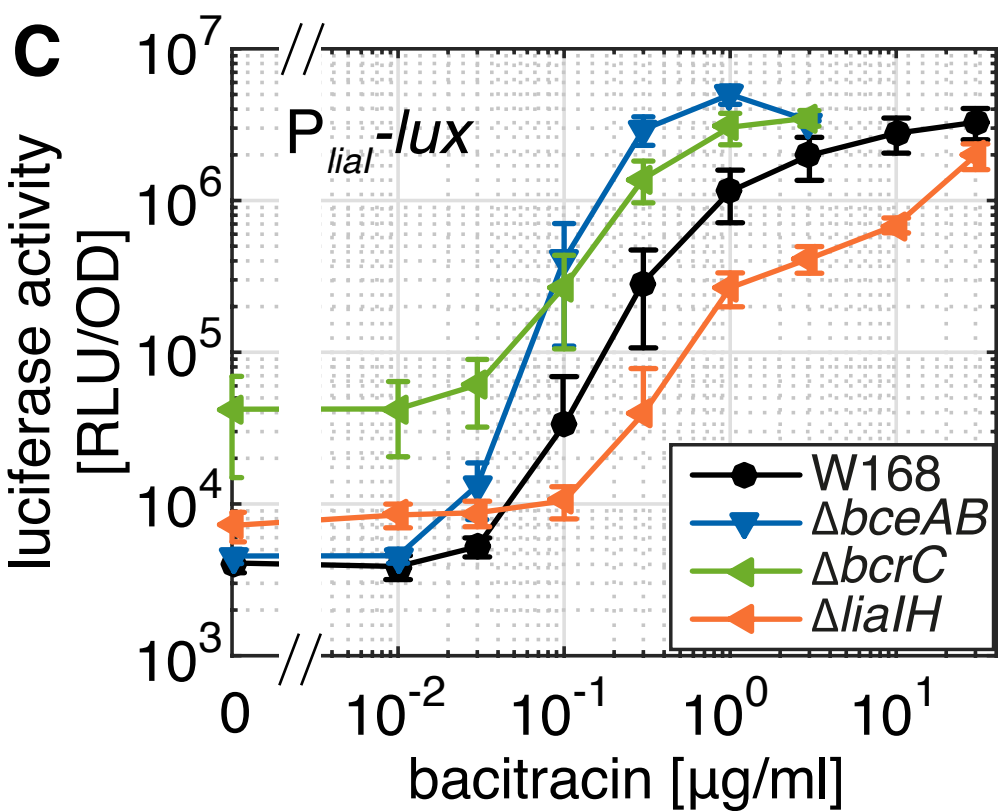
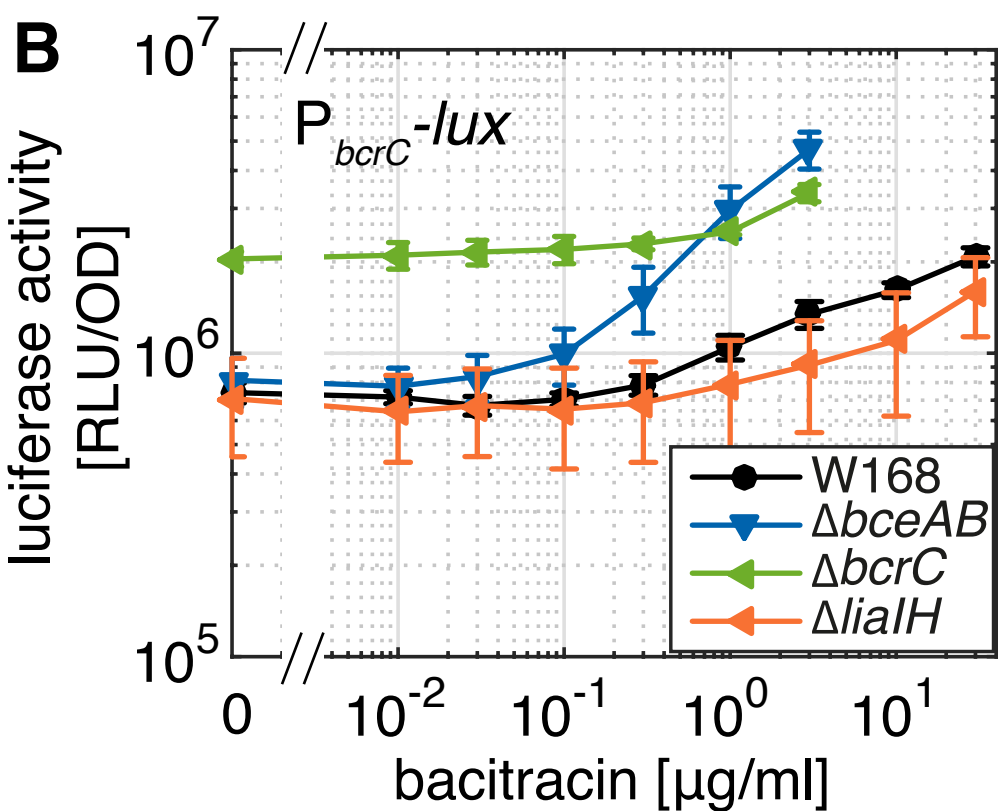
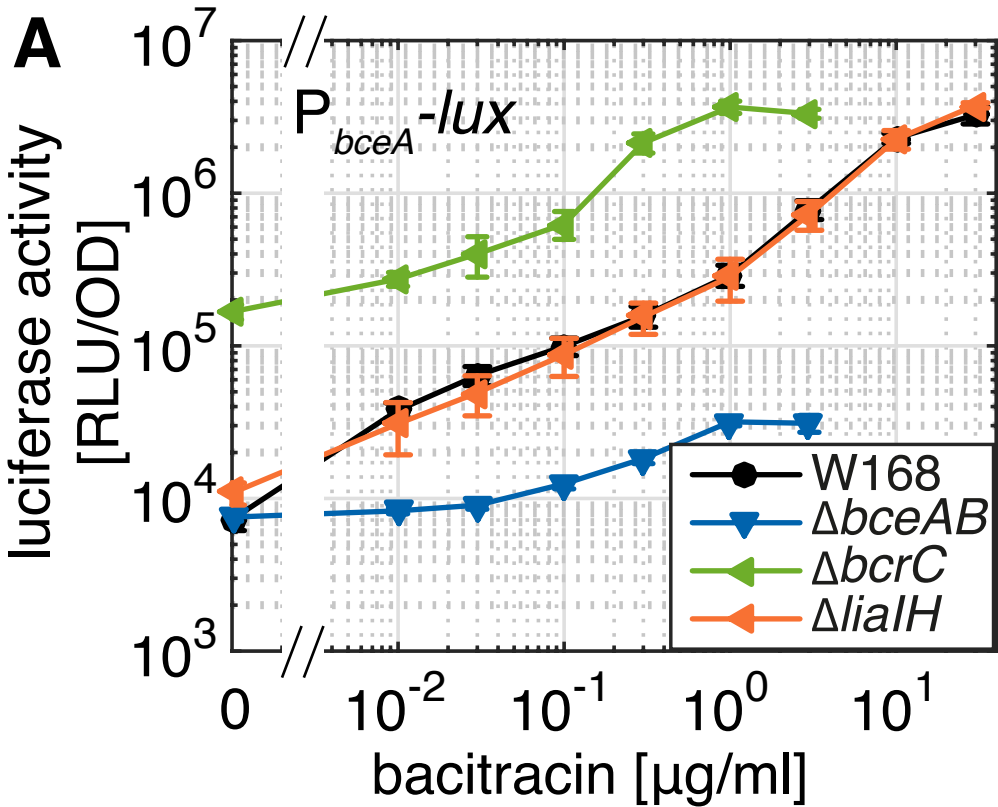
Figure 4. Regulatory crosstalk between primary and secondary resistance modules. Target promoter activities of P_{bceA} -*lux* and P_{lialH} -*lux* in strains expressing different levels of **(A)** BceAB, **(B)** BcrC and **(C)** LialH, as given by specific luciferase activity (RLU/OD₆₀₀) one hour after addition of indicated amounts of bacitracin. Measurements were performed as described in Figure 3. Colors code for different expression levels of resistance module X ($X = bceAB$, $bcrC$ or $lialH$), as driven by the xylose-inducible promoter P_{xyIA} : (*red*) No expression, via deletion of module X; (*orange*) Low constitutive expression, via complementation of the deletion mutant with P_{xyIA} -X in the absence of xylose; (*light green*) High constitutive expression, via complementation of the deletion mutant with P_{xyIA} -X in the presence of 0.2% xylose; (*dark green*) Overexpression in W168 wild type background, via expression of P_{xyIA} -X in the presence of 0.2% xylose. The corresponding strains are (A) TMB1619, TMB1623, TMB2590, TMB2594 (P_{bceA} -*lux*) and TMB1617, TMB1621, TMB2589, TMB2593 (P_{lialH} -*lux*) (B) TMB1619, TMB1627, TMB2592, TMB2430 (P_{bceA} -*lux*) and TMB1617, TMB1625, TMB2591, TMB2429 (P_{lialH} -*lux*) (C) TMB1619, TMB1661, TMB2693, TMB2691 (P_{bceA} -*lux*) and TMB1617, TMB1659, TMB2692, TMB2690 (P_{lialH} -*lux*), as listed in Table S1. Error bars indicate the standard deviation between at least three biological replicates.

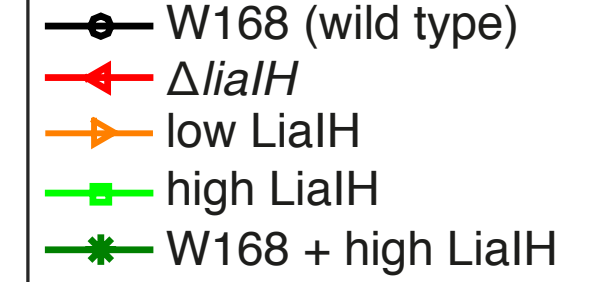
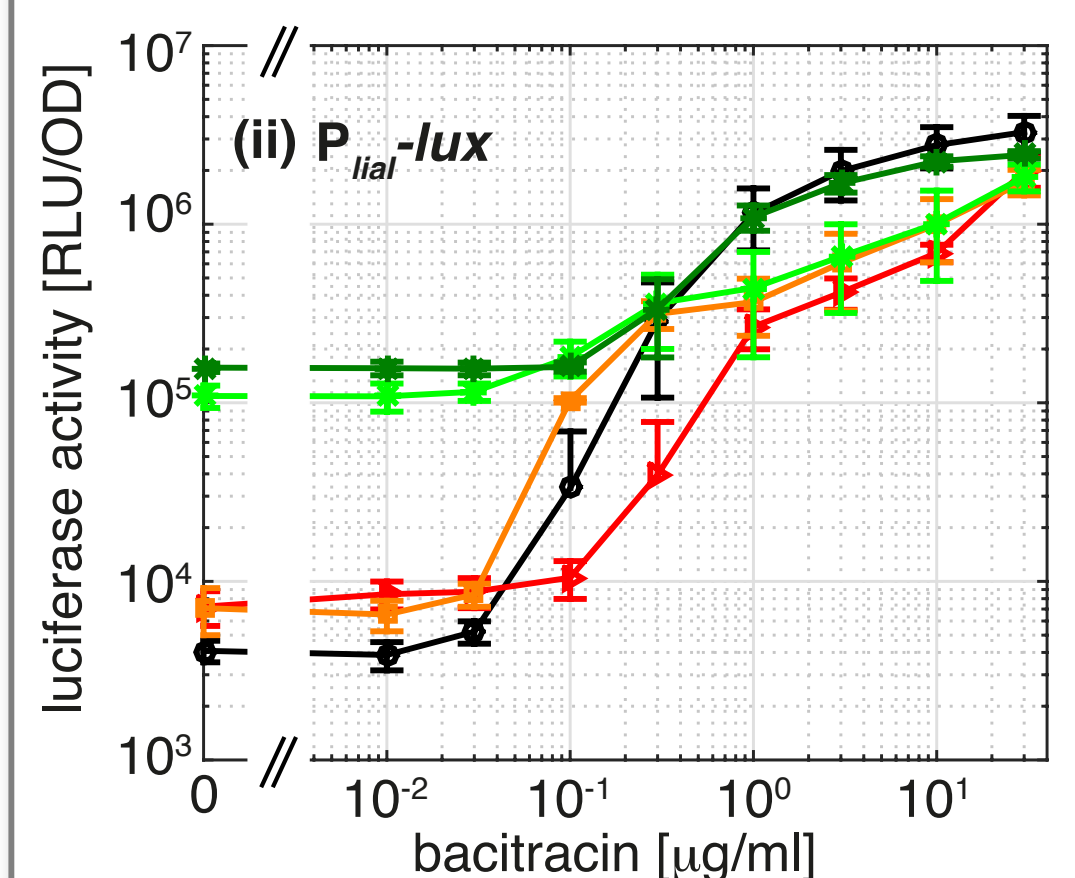
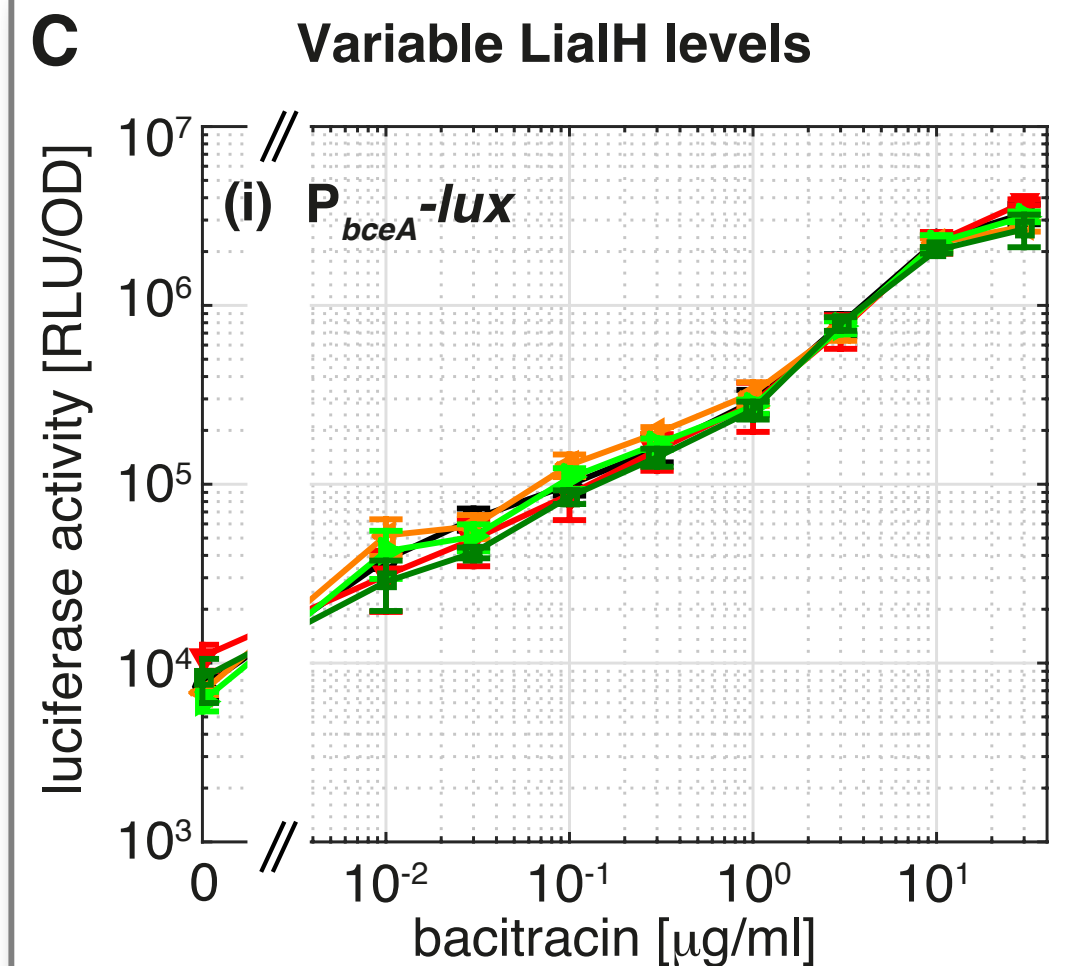
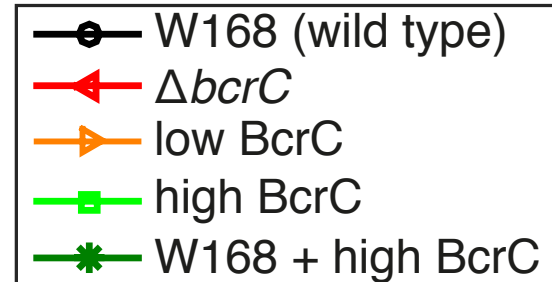
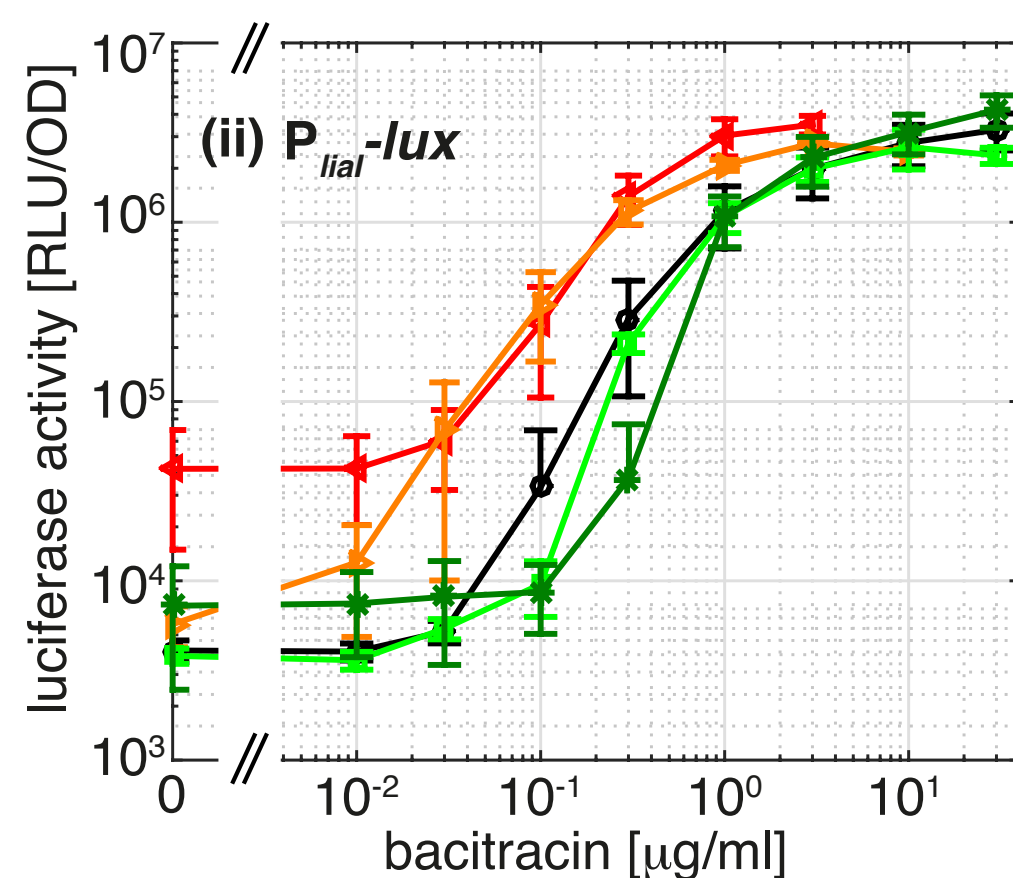
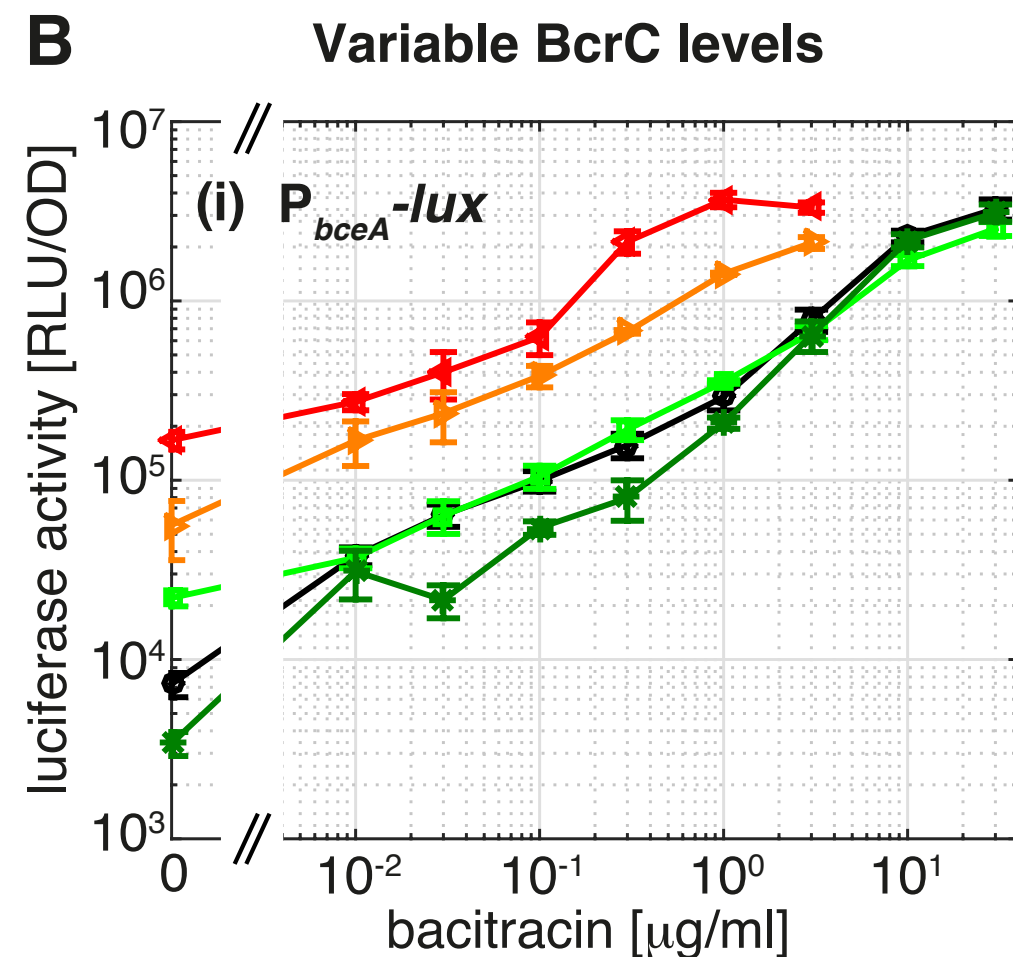
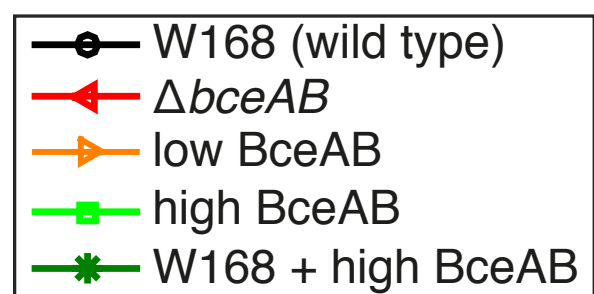
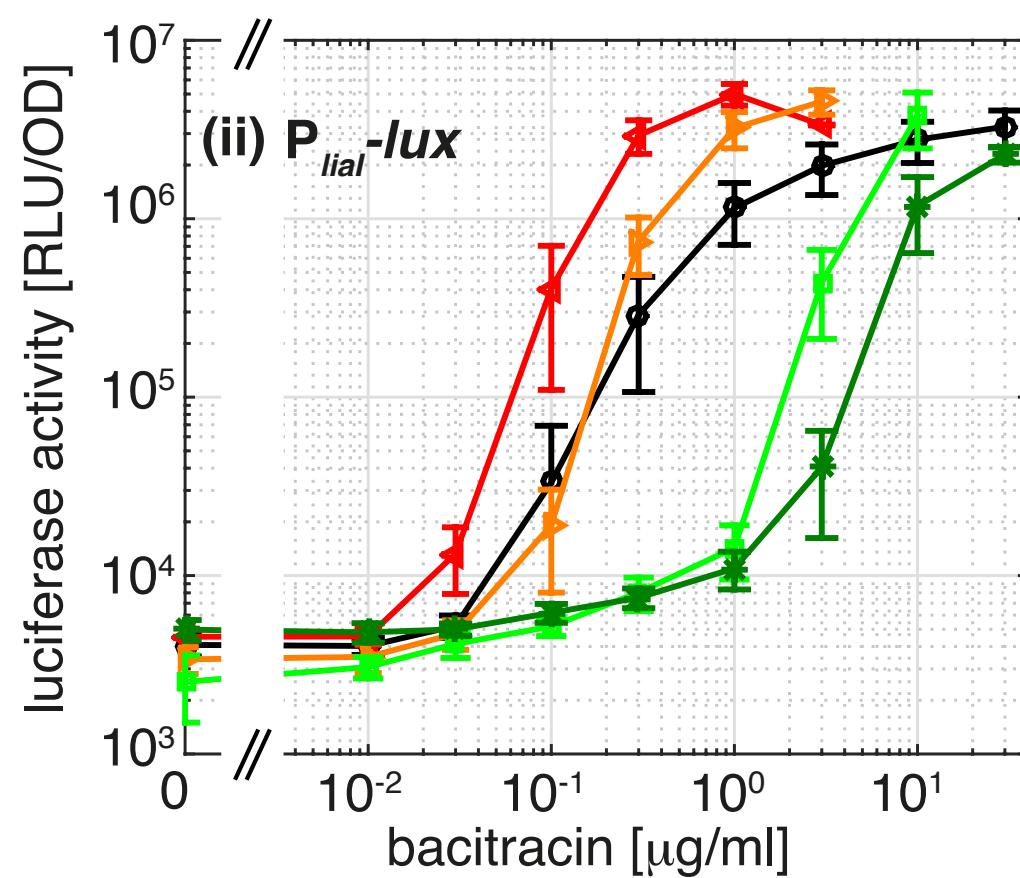
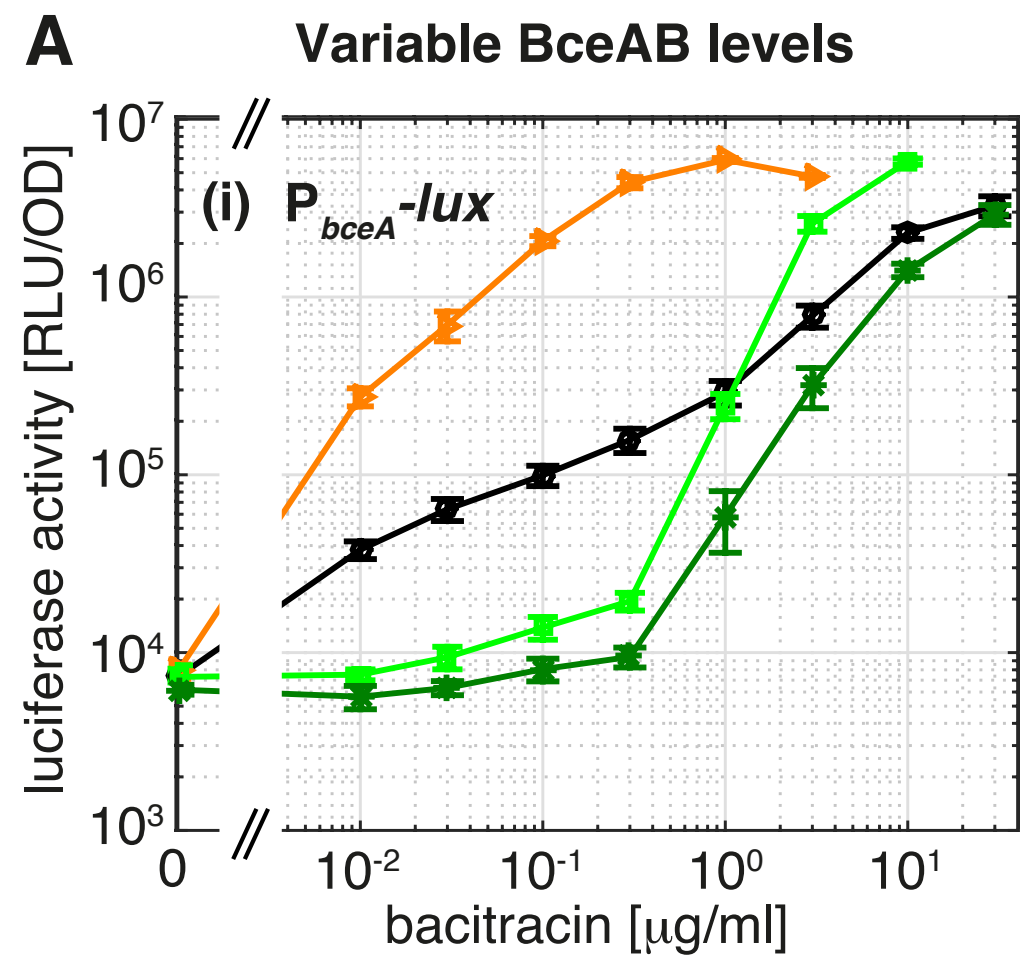
Figure 5. Noise in the response of bacitracin resistance modules. Single cell bacitracin response of wild type strains carrying **(A)** P_{bceA} -*gfp*, **(B)** P_{bcrC} -*gfp*, and **(C)** P_{lialH} -*gfp* reporter

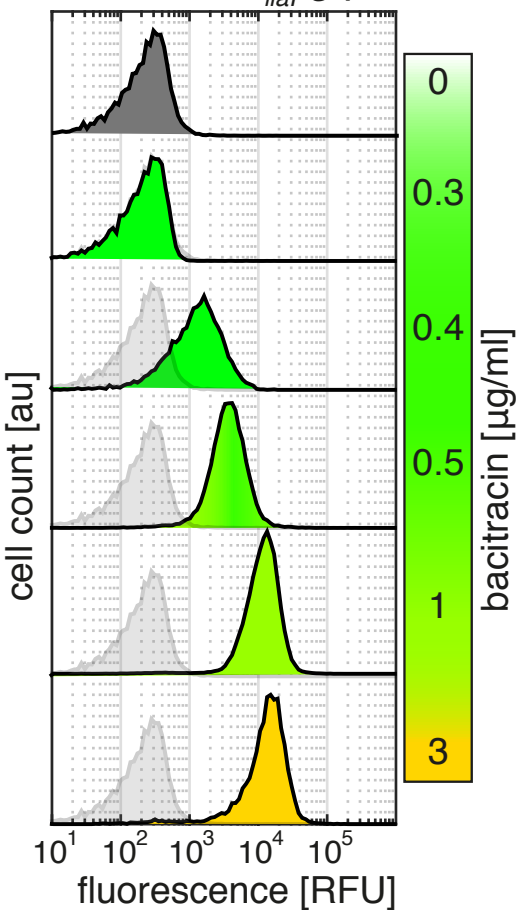
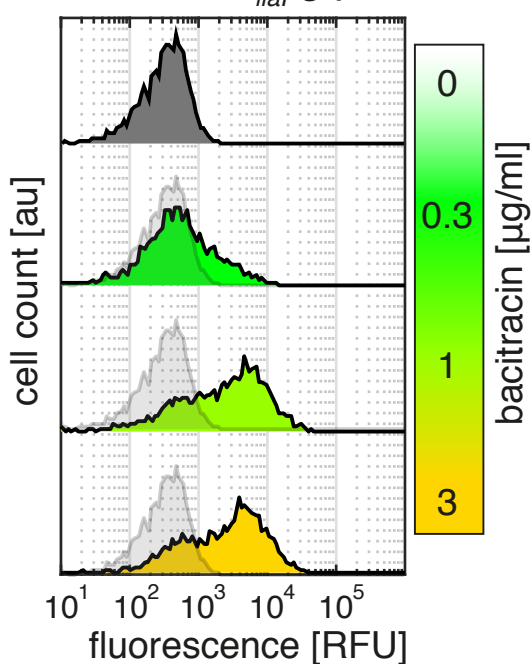
726 plasmids (strains TMB2174, TMB2173 and TMB1176, see Table S1), as well as in **(D)** $\Delta bceAB$
727 and **(E)** $\Delta bcrC$ mutant backgrounds carrying a P_{liaI} -*gfp* reporter plasmid (strains TMB2056 and
728 TMB2057, see Table S1). Fluorescence distributions were quantified using flow cytometry, one
729 hour after treatment of exponentially growing cells (37°C, LB medium) with bacitracin.
730 Fluorescence distributions (*colored*) were obtained under bacitracin treatment indicated on the
731 right, while transparent overlays (*gray*) are reference distributions obtained in the absence of
732 bacitracin treatment. In every case one representative dataset of at least two independent
733 biological replicates is shown.









A $\Delta bceAB$ P_{lial} -gfp**B** $\Delta bcrC$ P_{lial} -gfp**C**